PHYSICAL REVIEW B VOLUME 59, NUMBER 2 1 JANUARY 1999-II

Infrared studies of a $La_{0.67}Ca_{0.33}MnO_3$ single crystal: Optical magnetoconductivity in a half-metallic ferromagnet

A. V. Boris, N. N. Kovaleva, and A. V. Bazhenov
Institute of Solid State Physics, Chernogolovka, Moscow district, 142432, Russia

P. J. M. van Bentum and Th. Rasing
Research Institute for Materials and High Field Magnet Laboratory, University of Nijmegen, 6525 ED Nijmegen, The Netherlands

S-W. Cheong
Bell Laboratories, Lucent Technologies, Murray Hill, New Jersey 07974
and Department of Physics and Astronomy, Rutgers University, Piscataway, New Jersey 08855

A. V. Samoilov and N.-C. Yeh
Department of Physics, California Institute of Technology, Pasadena, California 91125
(Received 30 September 1998)

The infrared reflectivity of a $La_{0.67}Ca_{0.33}MnO_3$ single crystal is studied over a broad range of temperatures (78–340 K), magnetic fields (0–16 T), and wave numbers ($20-9000\,cm^{-1}$). The optical conductivity gradually changes from a Drude-like behavior to a broad peak feature near $5000\,cm^{-1}$ in the ferromagnetic state below the Curie temperature $T_C = 307$ K. Various features of the optical conductivity bear striking resemblance to recent theoretical predictions based on the interplay between the double exchange interaction and the Jahn-Teller electron-phonon coupling. A large optical magnetoconductivity is observed near T_C. [S0163-1829(99)50602-4]

Perovskite manganites of $R_{(1-x)}A_xMnO_3$ (R: trivalent rare-earth ions, A: divalent alkaline-earth ions, $0.2 \leqslant x \leqslant 0.5$) are materials with interesting electric and magnetic properties which give rise to phenomena such as the colossal negative magnetoresistance (CMR). Many structural,[1,2] magnetic,[3–5] and transport[6–8] aspects of a ferromagnetic (FM) metal-paramagnetic (PM) insulator instability, triggered by either temperature or external magnetic field, can be explained in terms of the interplay of the electron-phonon coupling and the double-exchange (DEX) transport mechanism.[9,10] A spin polarized half-metallic behavior exists in the ferromagnetic state, which is believed to be essential for the occurrence of CMR in the perovskite manganites.[11–14] However, details of the interplay between the Jahn-Teller (JT) type electron-phonon coupling and the DEX mechanism[9,10] are yet to be manifested experimentally.

This work aims at addressing this important issue by correlating the infrared (IR) optical conductivity of a $La_{0.67}Ca_{0.33}MnO_3$ single crystal with its magnetic and electron transport properties. The experimental approach involves measurements of the IR reflectivity spectra of a $La_{0.67}Ca_{0.33}MnO_3$ single crystal over a broad range of temperatures (78–340 K), magnetic fields (0–16 T), and wave numbers ($20-9000\,cm^{-1}$). In addition, dc magnetization and resistivity measurements are performed on the same sample for comparison. The observed temperature dependence of the optical conductivity bears striking resemblance to the theoretical predictions[9,10] of temperature-dependent competing effects between the JT coupling and the DEX interaction in the ferromagnetic state. The frequency dependence of the optical conductivity $\sigma(\omega)$ varies from the Drude-like behavior at low temperatures to a broad peak feature in the mid-IR at high temperatures. These characteristics of optical conductivity are shown to be determined by the ratio of the electron-phonon coupling to the electron kinetic energy, consistent with theory.[9,10]

The single crystal of $La_{0.67}Ca_{0.33}MnO_3$ was grown by a floating zone method. X-ray diffraction confirms that the sample is single-phased with an orthorhombic structure close to cubic. The temperature-dependent magnetization of this $La_{0.67}Ca_{0.33}MnO_3$ single crystal reveals that the Curie temperature T_C is at 307 K (± 1 K), and the resistivity $\rho(T)$ shows a monotonic decrease with decreasing temperature over the region investigated, with a significant change in the slope at T_C.

Near-normal incidence reflectivities were measured with a combination of a Fourier transform spectrometer, ''Bruker'' IFS 113v, and grating monochromator, to cover the frequency range from 20 to $25\,000\,cm^{-1}$. The far-IR reflectivity spectra were studied in the Faraday geometry over $20-800\,cm^{-1}$ by using a ''Bruker'' IFS 113v spectrometer equipped with a superconducting magnet of field strength up to 18.5 T. The reflectivities were calibrated against a reference Au mirror in the far-IR region, and against a reference Al mirror at higher frequencies.

The reflectivity spectra of the $La_{0.67}Ca_{0.33}MnO_3$ single crystal for different temperatures from above T_C down to 78 K and for wave numbers up to $9000\,cm^{-1}$ are shown in Fig. 1, with more details up to $800\,cm^{-1}$ given in the inset. The reflectivity spectra above T_C reveal three distinct optical phonon features near 170, 350, and $580\,cm^{-1}$. These features are interpreted as the cubic perovskite vibration bands of the F_{1u} symmetry.[15,16] As the temperature decreases from 340 to

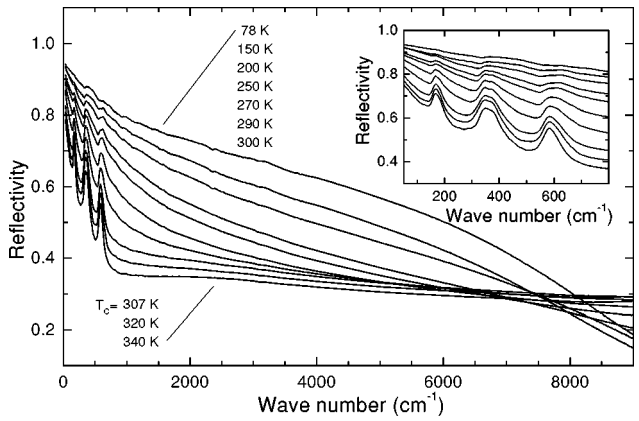

FIG. 1. The reflectivity spectra of the $La_{0.67}Ca_{0.33}MnO_3$ single crystal for different temperatures ($T_C = 307$ K). Inset: more details in the far-IR region.

78 K, the reflectivity displays a gradual increase, consistent with the occurrence of a metallic FM phase at low temperatures. The optical phonon modes evident above 250 K become screened and eventually disappear in the metallic phase.

To obtain the optical conductivity through the Kramers-Kronig analysis, we used a Hagen-Rubens extrapolation for the low-frequency region. Extrapolation towards high frequencies was made by using the reflectivity data of $La_{(1-x)}Sr_xMnO_3$ from 25 000 to 80 000 cm^{-1},[13] because these data are nearly independent of the temperature and doping level. For energies higher than 80 000 cm^{-1}, an extrapolation using the ω^{-4} frequency dependence was used. The real part of the optical conductivity $\sigma(\omega)$ for different temperatures from above T_C down to 78 K is shown in Fig. 2. The Drude approximation with a frequency-independent scattering rate is used to describe the data in the low-frequency limit, and a sum of Lorentz oscillator functions is used to account for the contribution from the transverse optical (TO) phonons and for the mid-IR bands. We find that at low temperatures ($T \leqslant 150$ K), the $\sigma(\omega)$ spectrum exhibits a

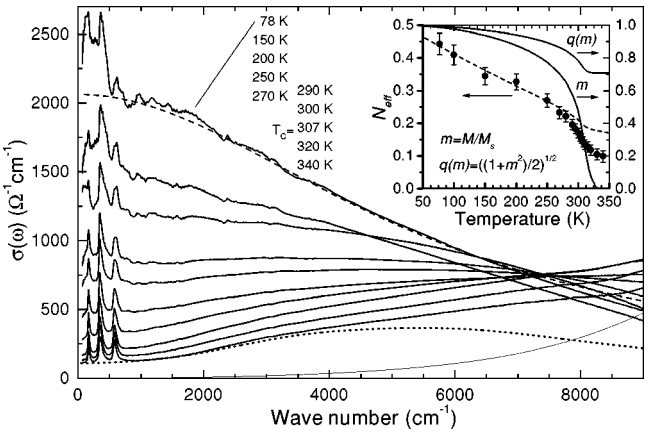

FIG. 2. The real part of the optical conductivity of the single crystal at different temperatures ($T_C = 307$ K). Inset: N_{eff} (closed circles), normalized dc magnetization at $H = 0.5$ T ($m = M/M_S$, $M_S \simeq 3.9\mu_B$), and the corresponding $q(m)$ (solid curves) vs temperature T. The suppression factor (see text) is illustrated by the dashed line.

dominant Drude-like contribution, yielding a plasma frequency $\omega_p \approx 2.6 \times 10^4$ cm^{-1}, a scattering rate $\gamma \approx 5.5 \times 10^3$ cm^{-1}, and a high-frequency dielectric constant $\varepsilon_\infty \approx 7.5$ at 78 K, as shown by the dashed line in Fig. 2. In the context of half-metallic ferromagnetism below T_C, these parameters provide an estimate for the majority carrier density per Mn, n, corrected by the effective mass, m^*, via the relation $nm_e/m^* = (\omega_p^2 m_e)/(4\pi N_{Mn} e^2) \approx 0.40-0.45$, where N_{Mn} is the number of Mn atoms per unit volume. Assuming an effective carrier concentration $n \simeq 2/3$ which is comparable to the doping level, we obtain a reasonable effective band mass $m^* \simeq 1.5-2m_e$.[17]

With increasing temperature, we find that the spectral weight of the Drude component gradually decreases. At temperatures above 250 K, the spectral weight is appreciably transferred to the broad mid-IR band. As shown in Fig. 2, the optical conductivity at $T \geqslant 250$ K exhibits a broad peak on a continuum, extending from the mid-IR region to the lowest frequencies. Well above T_C at $T = 340$ K the detailed dispersion analysis shows that the optical conductivity includes the small Drude part and broad mid-IR band around 5000 cm^{-1} resulting from the intraband electronic excitations near the Fermi level, as presented by the dotted line in Fig. 2. In addition, the mid-IR spectrum is completed with the broad band peaking at approximately 11 000 cm^{-1}, outside the range of the figure (as shown by the light solid line in Fig. 2), which appears in the PM phase and may be treated as a contribution from the interband excitations. In the inset of Fig. 2, we show the temperature dependence of the total spectral weight of the Drude and mid-IR contributions derived from the Drude-Lorentz analysis, expressed in terms of the effective electron density per Mn site:

$$N_{eff} = \frac{2m_e}{\pi e^2 N_{Mn}} \int [\sigma_{Drude}(\omega) + \sigma_{mid-IR}(\omega)]\, d\omega. \quad (1)$$

As shown in the inset of Fig. 2, N_{eff} is not a conserved quantity: It decreases monotonically with increasing temperature in the FM state, and then exhibits a sharp drop at the Curie temperature.

The experimental observation of the frequency-dependent optical conductivity may be understood in terms of a theoretical model that incorporates both the DEX transport mechanism and an electron-phonon coupling effect.[9] In a dynamical mean-field approximation, it is assumed that the d electron in the e_g orbital of the Mn^{3+} ion is coupled to $3t_{2g}$ spins of Mn ions via the Hund's rule exchange coupling, and to the classical oscillators of the lattice through the Jahn-Teller effect.[9] It is found that T_C, $\sigma(\omega,T)$, and $\rho(T)$ are functions of an effective coupling parameter λ, defined as the ratio of the energy gain from localizing an electron at the Mn site to the electron kinetic energy, t. That is, $\lambda \equiv E_{JT}/t$ and $E_{JT} = g^2/k$, where g is the electron-phonon coupling strength, k the force constant of the classical oscillators.[9] Comparing our data with Ref. 9, we find that the effective coupling parameter λ is comparable to unity, suggesting a moderate electron-phonon coupling in $La_{0.67}Ca_{0.33}MnO_3$. The broad peak in the mid-IR optical conductivity can be attributed to transitions between the two e_g orbitals of adjacent Mn sites, and is therefore comparable to the Jahn-Teller splitting. Comparing our optical conductivity data (which

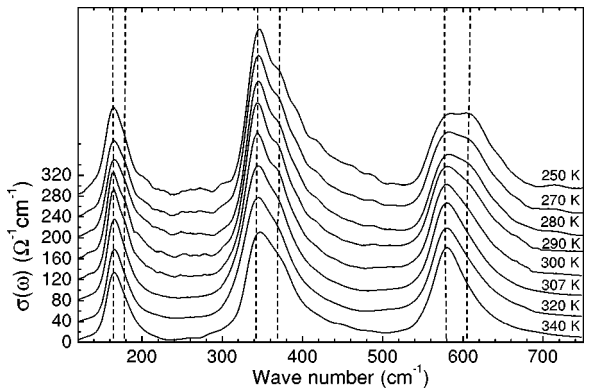

FIG. 3. Far-IR region of the real part of the reduced optical conductivity, derived by subtracting the electronic background at different temperatures: Successive curves are offset by $40\,\Omega^{-1}\,\mathrm{cm}^{-1}$ for clarity.

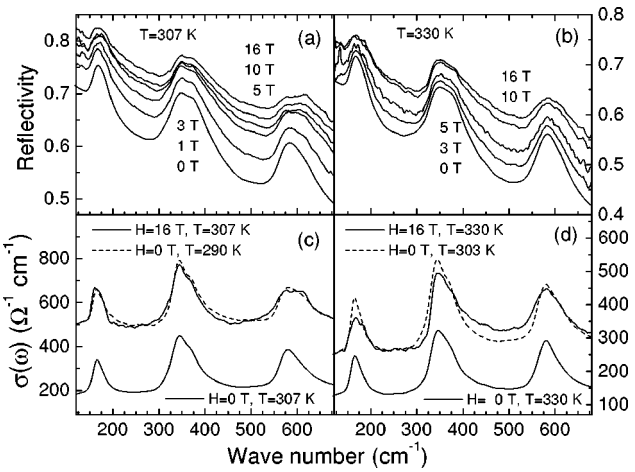

FIG. 4. (a), (b) The far-IR reflectivity spectra of the $La_{0.67}Ca_{0.33}MnO_3$ single crystal for different magnetic fields at (a) $T=307$ K; and (b) $T=330$ K. (c), (d) Comparison of the effect of applying an external magnetic field (16 T) and that of reducing the temperature on the far-IR optical conductivity in the single crystal at (c) $T=307$ K and (d) $T=330$ K.

display a broad peak at $\sim 5000\,\mathrm{cm}^{-1}$ near $T_C \approx 307$ K) with theoretical calculations of Ref. 9, we obtain a crude estimate of $t \sim E_{JT} \sim 0.3$ eV for $La_{0.67}Ca_{0.33}MnO_3$ single crystals. In accordance with the theory, the temperature-dependent spectral weight N_{eff} is proportional to the kinetic energy of mobile carriers. In the FM state, the effective hopping amplitude $t^{eff}(m)$ is dependent on the normalized magnetization $m = M/M_s$, and may be approximated by the expression $t^{eff}(m) \approx tq(m) \equiv t\sqrt{(1+m^2)/2}$.[18] Using a saturated magnetization $M_s \approx 3.9\mu_B$ for $La_{0.67}Ca_{0.33}MnO_3$ and the empirical magnetization data $M(T)$ of the sample, the resultant temperature-dependent m and $q(m)$ are illustrated in the inset of Fig. 2, along with N_{eff}. This comparison of N_{eff} and $q(m)$ shows that the decrease in N_{eff} with temperature cannot be entirely accounted for by the temperature dependence of $t^{eff}(m)$ alone. We may consider another temperature-dependent factor for N_{eff} due to the JT-induced suppression of the DEX interaction. This factor, estimated by the expression $\exp[-E_{JT}k_BT/(\hbar\omega_{ph})^2]$,[19] with ω_{ph} being a characteristic phonon frequency, is independent of the magnetization, unlike $t^{eff}(m)$. Combining the temperature dependence of both $q(m)$ and the exponential suppression factor, we obtain a consistent description for the spectral weight $N_{eff}(T)$ at temperatures below T_C, as shown by the dashed line in the inset of Fig. 2, with a reasonable fitting parameter $[E_{JT}/(\hbar\omega_{ph})^2] \sim 1/(0.045 \pm 0.005\,\mathrm{eV})$. Despite good agreement between our data and the theoretical analysis of Millis *et al.*[9] at $T < 250$ K, we note that $N_{eff}(T)$ begins to decrease faster with temperature than the theoretical prediction as T becomes closer to T_C. A sharp drop of N_{eff} at T_C suggests that the FM metal–PM insulator transition in the CMR manganites is associated with a fundamental change in the electronic configuration, which results in a significant shift in the spectral weight, from intraband excitations near the Fermi level in the FM state to effectively interband excitations in the PM state, the latter involving an excitation energy of the order of the Hund's rule exchange energy.[13]

Figure 3 shows the real part of the reduced optical conductivity at phonon frequencies, derived by subtracting the electronic background at different temperatures. The TO phonon spectra are represented by three sets of splitted bands and fitted by six Lorentzian line shapes with maxima at 164, 178, 343, 370, 579, and $605\,\mathrm{cm}^{-1}$. The vertical dashed lines in Fig. 3 show the temperature dependence of the frequencies for the main TO phonon modes derived by the dispersion analysis. No discernible changes in frequency are found in the TO phonon modes of the single crystal except for redistribution of oscillator strength within the splitted bands with decreasing temperature. This is in contrast to the report on polycrystalline $La_{0.7}Ca_{0.3}MnO_3$, where the fine structure of the phonon modes could not be resolved.[15] The observed redistribution of intensities between 579 and $605\,\mathrm{cm}^{-1}$ in favor of the high-frequency one is in qualitative agreement with the pulsed neutron-scattering data on powder samples of $La_{1-x}Sr_xMnO_3$, $0 \leqslant x \leqslant 0.4$.[2] As reported by Louca *et al.* the number of the MnO_6 Jahn-Teller distorted octahedra is decreased with decreasing temperature below T_C resulting in an increase of the average number of the short Mn-O lengths. This is consistent with the observed temperature variation (Fig. 3) of the phonon feature near $579\,\mathrm{cm}^{-1}$ related to the Mn-O bond length modulation.[15,16]

The magnetic-field effect on the optical conductivity is studied by measuring the far-IR reflectivity spectra under a wide range of magnetic fields (0–16 T). A gradual increase in the reflectivity for the entire far-IR frequency range is observed as the external magnetic field increases from 0 to 16 T and for all temperatures above T_C [as shown in Figs. 4(a) and 4(b) for 307 and 330 K]. To compare the temperature and magnetic-field effect in detail, we consider representative spectra shown in Figs. 4(c) and 4(d). The reference optical conductivity spectrum in zero field and for a constant temperature is presented by the lower solid curve in each panel. The upper solid curve represents the spectrum taken in the maximum field $H=16$ T and at a temperature equal to that of the reference spectrum. The dashed curve in each panel corresponds to the optical conductivity spectrum at a temperature lower than that of the reference spectrum, with the same low-frequency limit as the upper solid curve. First, we note that in the vicinity of T_C, [i.e., at $T=307$ K, see Fig. 4(c)], the effect on enhancing the optical conductivity due to an external magnetic field (16 T) is found to be comparable

to that due to decreasing the temperature (by $\Delta T = 17\,\mathrm{K}$) in the entire far-IR frequency range. We estimate that the corresponding dimensionless scaling factor $k_B \Delta T / \mu_B H$ gradually changes with increasing temperature from ≈ 1.6 at T_C to ≈ 2.5 at $T = 330\,\mathrm{K}$, as follows from Figs. 4(c) and 4(d). We also note the significant increase of $\sigma(\omega)$, as illustrated in Figs. 4(a)–4(d), with the increasing magnetic field. The magnetoconductivity, as large as about 50% at 5 T in the vicinity of the Curie temperature, is observed and may be referred to as an optical CMR effect.

In summary, we find that the optical conductivity spectra of a $La_{0.67}Ca_{0.33}MnO_3$ single crystal manifest a crossover from the Drude-like to a hopping conductivity below the FM to PM phase transition. The spectral features are in good qualitative agreement with recent theoretical predictions based on the interplay between the double-exchange mechanism and the Jahn-Teller type electron-phonon coupling. The optical conductivity and the dc magnetization and resistivity data are consistent with a moderate effective electron-phonon coupling.[9] A large optical magnetoconductivity at the phonon frequencies is reported.

This research at the Institute of Solid State Physics is supported by Russian State Program under Grant No. 96031. Part of the work done at Caltech is supported by NASA/OSS and the Packard Foundation.

[1] P. G. Radaelli *et al.*, Phys. Rev. B **54**, 8992 (1996).
[2] D. Louca *et al.*, Phys. Rev. B **56**, R8475 (1997).
[3] M. R. Ibarra *et al.*, Phys. Rev. Lett. **75**, 3541 (1995).
[4] A. Shengelaya *et al.*, Phys. Rev. Lett. **77**, 5296 (1996).
[5] S. B. Oseroff *et al.*, Phys. Rev. B **53**, 6521 (1996).
[6] S. G. Kaplan *et al.*, Phys. Rev. Lett. **77**, 2081 (1996).
[7] M. Jaime *et al.*, Phys. Rev. B **54**, 11 914 (1996).
[8] G.-M. Zhao *et al.*, Nature (London) **381**, 676 (1996).
[9] A. J. Millis, R. Mueller, and B. I. Shraiman, Phys. Rev. B **54**, 5405 (1996).
[10] H. Roder, Jun Zang, and A. R. Bishop, Phys. Rev. Lett. **76**, 1356 (1996); J. Zhang, A. R. Bishop, and H. Roder, Phys. Rev. B **53**, R8840 (1996).
[11] W. E. Pickett and D. J. Singh, Phys. Rev. B **53**, 1146 (1996).
[12] H. Y. Hwang *et al.*, Phys. Rev. Lett. **77**, 2041 (1996).
[13] Y. Okimoto *et al.*, Phys. Rev. B **55**, 4206 (1997).
[14] J. Y. T. Wei, N.-C. Yeh, and R. P. Vasquez, Phys. Rev. Lett. **79**, 5150 (1997).
[15] K. H. Kim *et al.*, Phys. Rev. Lett. **77**, 1877 (1996).
[16] A. V. Boris *et al.*, J. Appl. Phys. **81**, 5756 (1997).
[17] The low-frequency optical conductivity may be approximated by the expression $\sigma(\omega \to 0) = \omega_p^2/(4\pi\gamma)$, and $\omega_p^2 \sim 1/m^*$. We attribute the small value of $\sigma(0) \approx 2000\,\mathrm{cm}^{-1}$ to the overdamping in the system, with $(\omega_p/\gamma) \sim 4.5$, rather than to a large effective mass $m^* \sim 80 m_e$ as reported in Ref. 13.
[18] A. J. Millis, P. B. Littlewood, and B. I. Shraiman, Phys. Rev. Lett. **74**, 5144 (1995); A. J. Millis *et al.*, *ibid.* **77**, 175 (1996).
[19] K. I. Kugel' and D. I. Khomskii, Usp. Fiz. Nauk **136**, 621 (1982) [Sov. Phys. Usp. **25**, 231 (1982)].